ARTHRITIS & RHEUMATISM
Vol. 56, No. 6, June 2007, pp 1817–1826
DOI 10.1002/art.22706

The Role of Vascular Cell Adhesion Molecule 1/ Very Late Activation Antigen 4 in Endothelial Progenitor Cell Recruitment to Rheumatoid Arthritis Synovium

Matthew D. Silverman,[1] Christian S. Haas,[1] Ali M. Rad,[2] Ali S. Arbab,[2] and Alisa E. Koch[3]

Objective. **Marrow-derived endothelial progenitor cells (EPCs) are important in the neovascularization that occurs in diverse conditions such as cardiovascular disorders, inflammatory diseases, and neoplasms. In rheumatoid arthritis (RA), synovial neovascularization propels disease by nourishing the inflamed and hyperproliferative synovium. This study was undertaken to investigate the hypothesis that EPCs selectively home to inflamed joint tissue and may perpetuate synovial neovascularization.**

Methods. **In a collagen-induced arthritis (CIA) model, neovascularization and EPC accumulation in mouse ankle synovium was measured. In an antibody-induced arthritis model, EPC recruitment to inflamed synovium was evaluated. In a chimeric SCID mouse/human synovial tissue (ST) model, mice were engrafted subcutaneously with human ST, and EPC homing to grafts was assessed 2 days later. EPC adhesion to RA fibroblasts and RA ST was evaluated in vitro.**

Results. **In mice with CIA, cells bearing EPC markers were significantly increased in peripheral blood and accumulated in inflamed synovial pannus. EPCs were 4-fold more numerous in inflamed synovium from mice with anti–type II collagen antibody–induced arthritis versus controls. In SCID mice, EPC homing to RA ST was 3-fold greater than to normal synovium. Antibody neutralization of vascular cell adhesion molecule 1 (VCAM-1) and its ligand component α4 integrin potently inhibited EPC adhesion to RA fibroblasts and RA ST cryosections.**

Conclusion. **These data demonstrate the selective recruitment of EPCs to inflamed joint tissue. The VCAM-1/very late activation antigen 4 adhesive system critically mediates EPC adhesion to cultured RA fibroblasts and to RA ST cryosections. These findings provide evidence of a possible role of EPCs in the synovial neovascularization that is critical to RA pathogenesis.**

Neovascularization is a hallmark of diverse pathologic conditions, including rheumatoid arthritis (RA) (1). Microcirculatory expansion occurs either through angiogenesis (the proliferation and branching off of preexisting microvessels) (2) or by vasculogenesis (the de novo formation of blood vessels from circulating endothelial progenitor cells) (EPCs) (3). Until recently, neovascularization in adult tissue was thought to occur exclusively through angiogenesis. The identification of circulating bone marrow–derived EPCs (4) has resulted in reevaluation of this classic paradigm of blood vessel development.

The pathogenesis of RA is critically dependent on neovascularization of the synovium, with microvascular expansion occurring before clinical symptoms appear (5). Synovial neovascularization is of pivotal importance in the progression of RA, in that it creates a direct conduit for the entry into the joint of circulating leukocytes that exacerbate inflammation, and provides nutrients to the hyperproliferative synovium.

Dr. Silverman's work was supported by the NIH (National Institute of Arthritis and Musculoskeletal and Skin Diseases institutional training grant AR-07080) and by American Heart Association postdoctoral fellowships (0425749Z and 0625748Z). Dr. Haas' work was supported by an American Heart Association postdoctoral fellowship (0423758Z). Dr. Arbab's work was supported by the Henry Ford Hospital Foundation (grant FHFH-A30864). Dr. Koch's work was supported by the Veterans Administration Research Services, by the NIH (grants AI-40987, HL-58695, and AR-48267), and by a Frederick G. L. Huetwell and William D. Robinson Professorship at the University of Michigan.

[1]Matthew D. Silverman, PhD, Christian S. Haas, MD (current address: University of Tuebingen, Tuebingen, Germany): University of Michigan Health System, Ann Arbor; [2]Ali M. Rad, MD, Ali S. Arbab, MD, PhD: Henry Ford Health System, Detroit, Michigan; [3]Alisa E. Koch, MD: University of Michigan Health System, and Department of Veterans Affairs, Ann Arbor, Michigan.

Address correspondence and reprint requests to Matthew D. Silverman, PhD, University of Michigan Health System, Internal Medicine Department, BRSB/Room 4388, 109 Zina Pitcher Road, Ann Arbor, MI 48109-2200. E-mail: mdsilver@med.umich.edu.

Submitted for publication July 31, 2006; accepted in revised form March 7, 2007.

EPCs have been described to accumulate in the synovial pannus in RA (6). Explorations into the molecular mechanisms by which EPCs are recruited from the circulation to inflamed tissue remain limited, however. In this study we demonstrated EPC homing to diseased synovium in several models of inflammatory arthritis. Our findings provide evidence of a primary role of the vascular cell adhesion molecule-1 (VCAM-1)/α4 integrin ligand/receptor pair in mediating the adhesive interactions between EPCs and inflamed synovial tissue and cells.

MATERIALS AND METHODS

Materials. Polyclonal sheep anti-human intercellular adhesion molecule 1 (ICAM-1) and VCAM-1 and goat anti-human ICAM-2 and LYVE-1 (a lymphatic endothelial cell–specific marker) were from R&D Systems (Minneapolis, MN). Mouse monoclonal antibodies against human α4, αL, and β2 integrins, and recombinant human tumor necrosis factor α (TNFα) were also from R&D Systems. Rabbit anti-human von Willebrand factor (vWF) antibody was from Dako (Carpinteria, CA). Fluorescein isothiocyanate (FITC)– or phycoerythrin (PE)–conjugated mouse anti-human monoclonal antibodies for flow cytometric analysis of α4, αL, and β2 integrins, CD3, CD4, CD8, CD14, CD19, CD31, and CD34, rat anti-mouse monoclonal antibody CD117, stem cell antigen 1 (Sca-1), and appropriate fluorescence-conjugated control antibodies were from BD PharMingen (San Diego, CA). PE-conjugated mouse anti-human CD133 was from Miltenyi Biotec, (Auburn, CA). Fetal bovine serum (FBS), RPMI 1640 culture medium, and phosphate buffered saline (PBS) were from Invitrogen (Carlsbad, CA). Chicken type II collagen and Freund's complete adjuvant were from Chondrex (Redmond, WA). Carboxyfluorescein diacetate succinimidyl ester (CFSE) was from Molecular Probes (Eugene, OR). All other reagents were from Sigma (St. Louis, MO).

Animals. DBA/1J mice were from Jackson Laboratories (Bar Harbor, ME). BALB/c and SCID/NCr mice were from the National Cancer Institute (Bethesda, MD). Animals were maintained on a 12-hour light/12-hour dark cycle, and received food and water ad libitum. Animal studies were conducted under approval of the University of Michigan's University Committee on Use and Care of Animals.

Endothelial progenitor cells. Human cells and tissue samples were obtained according to University of Michigan and/or Henry Ford Health System Institutional Review Board–approved protocols. CD133+ leukocytes were purified from cord blood obtained from anonymous donors within 24 hours postpartum, using an immunomagnetic cell isolation kit (Miltenyi Biotec). Human CD34+ cells were obtained from the National Disease Research Interchange (Philadelphia, PA). Enriched human EPCs were >95% CD133+, as determined by flow cytometry. Mouse progenitor cells, determined based on their lack of expression of lineage markers (Lin−), were isolated from bone marrow from femurs, tibias, and humeri of 6-week-old-male DBA/1J or BALB/c mice, using a hematopoietic cell isolation kit (Stem Cell Technologies, Vancouver, British Columbia, Canada). EPCs were used immediately or were expanded up to 30-fold in culture, using StemSpan progenitor cell media (Stem Cell Technologies) containing 50 ng/ml recombinant human Flt-3 ligand, 50 ng/ml recombinant human stem cell factor, and 50 ng/ml recombinant human thrombopoietin (Stem Cell Technologies).

Synovial tissue and RA synovial fibroblast cultures. RA synovial tissue (ST) was obtained from patients undergoing arthroplasty or synovectomy. Normal ST was obtained at autopsy or from patients undergoing amputation, within 24 hours after death or limb removal, respectively. For studies of EPC adhesion to ST, tissue specimens were snap-frozen in liquid nitrogen using OCT embedding medium (Sakura, Torrance, CA), and were cut into 8-μm cryosections just before use. For mouse engraftment studies, ST samples were cut into 5-mm^3 sections under aseptic conditions and were cryopreserved in liquid nitrogen in 20% DMSO–80% FBS until used in experiments. Human RA synovial fibroblasts were isolated from RA ST using a solution of Dispase (2.4 mg/ml), type II collagenase (250 units/ml), and DNase (1×10^4 units/ml) in PBS, cultured in RPMI 1640 containing 10% FBS and 2 m*M* L-glutamine, and used between passages 6 and 9.

Flow cytometry. After blocking in PBS containing 20% FBS, EPCs (1×10^5–1×10^6) were stained in 200 μl blocking buffer containing a 1:50 dilution of the appropriate FITC- or PE-conjugated antibodies. To evaluate nonspecific antibody binding and for flow cytometer compensation adjustment, EPC samples were separately stained with isotype-matched fluorochrome-conjugated control antibodies, at the same concentration/reaction volume as test samples. After staining, EPCs were evaluated on an Epics XL flow cytometer (Beckman Coulter, Miami, FL). At least 10^4 events were recorded for each sample, and all experiments were repeated at least 3 times.

Immunohistochemistry. Ankle cryosections from mice with collagen-induced arthritis (CIA) were stained for vWF, LYVE-1, or CD117 (c-Kit). For CD117 and LYVE-1 staining, cryosections were blocked in Tris buffered saline (TBS) containing 20% FBS. Primary antibodies were added for 30 minutes at 10 μg/ml, followed by washing in TBS–0.1% Tween 20 (TBST). Appropriate alkaline phosphatase–conjugated secondary antibodies (Sigma) were added for 30 minutes at 1:100 dilutions in TBS, followed by TBST washing and addition of the chromogenic substrate fast red (Pierce, Rockford, IL). Sections were hematoxylin counterstained and evaluated by brightfield microscopy. For vWF staining of blood vessels, formalin-fixed, decalcified, paraffin-embedded sections of mouse ankles were antigen-retrieved using a combination of heat treatment (20 minutes at 80°C) (Target Retrieval Solution; Dako), and protease K treatment (10 μg/ml in 10 m*M* Tris HCl/1 m*M* EDTA [pH 8.0], for 20 minutes at 37°C). After antigen retrieval, sections were washed with TBST, and the staining protocol was resumed at the blocking step. For assessment of vWF-positive blood vessel density, the mean value from >10 sections per animal (n = 14 hind limbs with grade 3 arthritis and 4 control hind limbs) was determined at the tibial/tarsal apposition. Micrographs of these sections were simultaneously assessed for maximal synovial thickness at the tibial/tarsal diarthrosis.

Collagen-induced arthritis. Female DBA/1J mice (6–8 weeks old) were injected intradermally at the base of the tail with 100 μl of a homogenized mixture of equal parts of chicken type II collagen (2 mg/ml) dissolved in 0.05*M* acetic acid, and Freund's complete adjuvant containing 4 mg/ml heat-killed

Mycobacterium tuberculosis. On day 21, mice were boosted with an intraperitoneal injection of 100 μg chicken type II collagen. Arthritis severity was scored daily after the boosting injection, by 1 or more observers, under blinded conditions. The scoring system ranks arthritis on a score of 0 (no symptoms) to 3 (maximal inflammation) per assessed ankle (7). Mice were killed at various time points between the day of arthritis onset and 40 days post–symptom development. Paws were formalin fixed or were cryopreserved in liquid nitrogen. In some cases, peripheral blood was drawn for EPC analysis, at the time mice were killed.

Antibody-induced arthritis. Eight week-old female BALB/c mice were injected intraperitoneally with 200 μl of a cocktail containing 1 mg each of 4 different anti–type II collagen monoclonal antibodies (Chemicon, Temecula, CA). Three days later, animals were boosted with an intraperitoneal injection of 50 μg lipopolysaccharide (LPS) in PBS. In this model, animals develop arthritis 1–2 days after receiving LPS, with maximal symptoms observed 5–7 days after LPS administration. Two days after the LPS injection, animals received an intravenous injection of 1×10^6 PKH26-labeled murine EPCs in 200 μl PBS. Control animals received vehicle injections. Cells were allowed to circulate for 5 days, animals were killed, and hind legs were snap frozen. Mouse ankle cryosections were assessed for EPC accumulation in the tibial/tarsal synovium by fluorescence microscopy, using a BX51 fluorescence microscope with DP Manager imaging software (Olympus, Melville, NY). At least 10 high-power fields (hpf) of 6 16-μm–thick sections were evaluated per animal. Only hind legs were evaluated in this model, since the joints are larger than in the front legs, and the synovium is more easily discernable.

SCID mouse/human ST chimera model. To observe human EPC homing to human ST in an in vivo model, we engrafted 0.5-mm^3 pieces of either normal or RA human ST subcutaneously on the backs of female 6-week-old SCID/NCr mice. ST was engrafted for ~2 weeks, after which 1×10^6 PKH26-labeled human CD34+ cells or EPCs (CD133+ cells) were injected intravenously. Cells were allowed to circulate for 2 days, animals were killed, excised grafts were snap frozen, and cryosections were evaluated for EPC accumulation by fluorescence microscopy. At least 10 hpf of between 4 and 9 16-μm–thick sections were evaluated per animal.

Enzyme-linked immunocellular assay. Confluent RA ST fibroblast monolayers, cultured in 96-well tissue culture plates, were treated with TNFα for up to 24 hours. At the end of the experiment, cells were fixed in 0.5% glutaraldehyde/RPMI base medium, washed in PBS, and evaluated for VCAM-1 and ICAM-1 cell surface expression by enzyme-linked immunocellular assay, as described previously (8). Results are presented as arbitrary fluorescence units or as a percentage of the indicated control (set at 100%). Background fluorescence from wells in which the primary antibody was omitted served as a control and was subtracted from experimental values. Conditions were replicated in 4–6 wells per experiment.

Western blot analysis. Western blotting for VCAM-1 and ICAM-1 was performed on lysates from TNFα-stimulated RA ST fibroblasts from 3 donors. Lysates were subjected to sodium dodecyl sulfate–polyacrylamide gel electrophoresis, proteins were transferred to nitrocellulose, and membranes were probed with VCAM-1 or ICAM-1 antibodies, followed by probing with horseradish peroxidase–conjugated secondary antibodies and development by chemiluminescence (Amersham, Arlington Heights, IL). Immunoblots were reprobed with rabbit anti-human β-actin (Sigma) for normalization. After digitization, band intensities were evaluated with UN-Scan-It software (Silk Scientific, Orem, UT). Band intensity corresponded to the sum of all pixel values in the selected region minus the background pixel value, and is presented as a ratio of VCAM-1 or ICAM-1 intensity to β-actin intensity.

EPC adhesion to cultured RA ST fibroblasts. Confluent RA ST fibroblast monolayers in 96-well tissue culture plates were stimulated with TNFα in various concentrations and for various lengths of time. RA ST fibroblasts were washed 3 times with RPMI–1% FBS. CFSE-labeled EPCs (50,000/well) were adhered to RA ST fibroblasts in medium in 100 μl/well for 20 minutes. In some experiments, neutralizing antibodies against adhesion molecules and integrins were mixed with the EPC suspension immediately prior to the adhesion assay. Nonadherent EPCs were washed off with media, and bound EPCs were quantified by measuring their fluorescence using 485/530-nm excitation/emission wavelength filters. RA ST fibroblast background autofluorescence was subtracted from all experimental values. Conditions were replicated in 4–6 wells per experiment.

EPC adhesion to ST cryosections. RA ST cryosections (8 μm) were rehydrated and overlaid with PKH26-tagged EPCs in RPMI–1% FBS (150 μl per section of a cell suspension of 50×10^5 EPCs/ml) that had been pretreated for 15 minutes with neutralizing sheep anti–VCAM-1, mouse anti–α4 integrin monoclonal antibody, or the appropriate control IgG (all at 10 μg/ml). After 15 minutes, nonattached EPCs were removed, and adherent EPCs in each section were counted by fluorescence microscopy (9), under blinded conditions, in 5 hpf (200× magnification), and the results averaged. Results are presented as the percentage of maximal binding (100% [number of adherent EPCs/hpf in the presence of control IgG antibody]).

Statistical analysis. Mean ± SEM values were calculated. The significance of differences in mean values between experimental and control groups was determined by Student's *t*-test. *P* values less than 0.05 were considered significant. Linear regression was used to obtain goodness-of-fit (r^2) values.

RESULTS

Isolation and characterization of EPCs. Enriched murine EPCs were consistently ≥95% Lin−. The EPC population (Lin−,Sca-1+,CD117+) was enriched >10-fold, from ~2% of total starting marrow cells to 25% (results not shown). We further characterized these EPCs, by flow cytometry, as being ~20% vascular endothelial growth factor receptor 2 positive, 75% CD31+, and 50% CD34+, consistent with expectations for an enriched angioblast subset. With isolation of cord blood CD133+ EPCs, we typically obtained 1×10^6 CD133+ EPCs per preparation, with a purity of ≥95%. More than 90% of these cells expressed both CD34 and CD31 on their surfaces, by flow cytometry, and these cells were uniformly negative for the leukocyte matura-

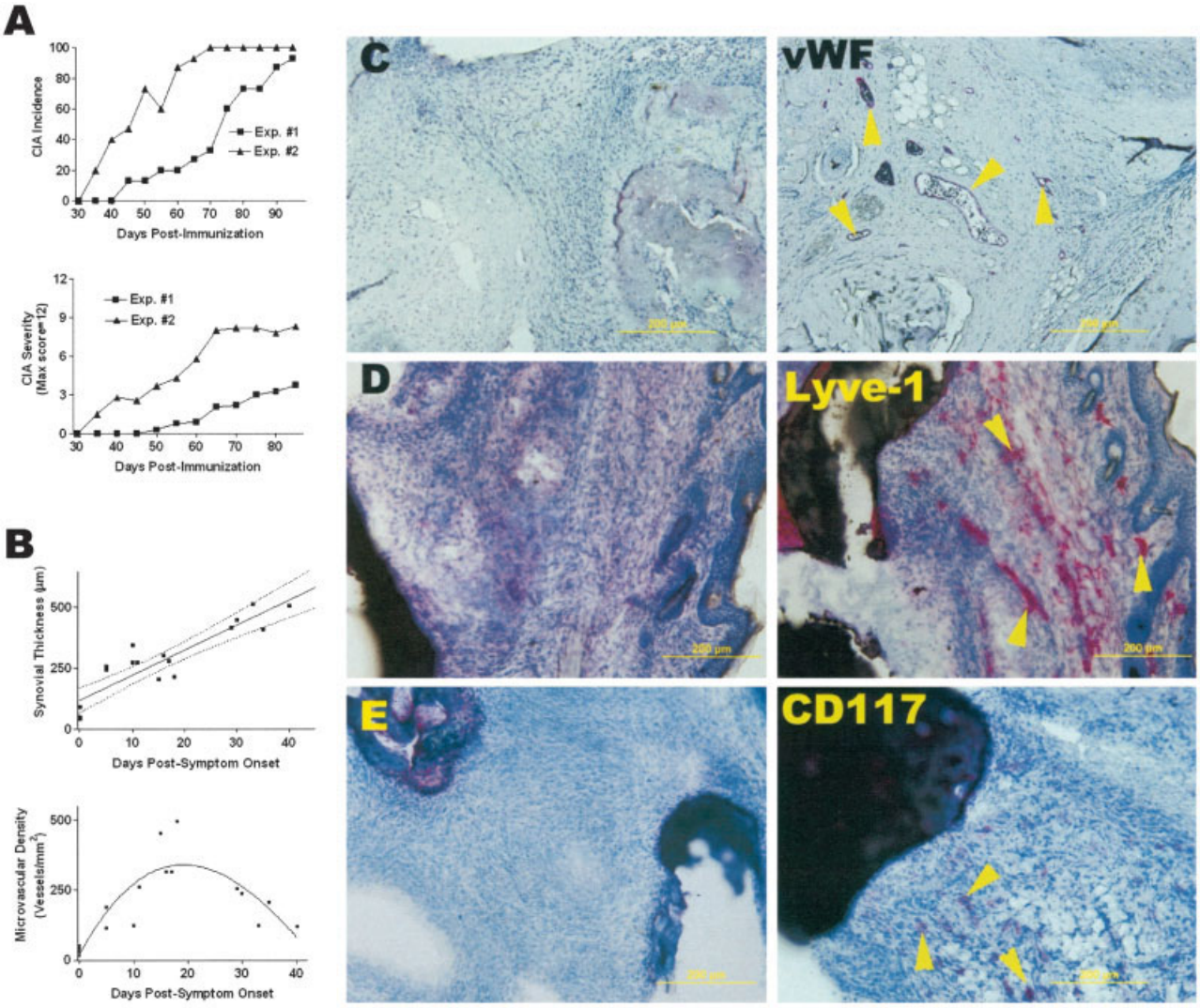

Figure 1. Neovascularization in collagen-induced arthritis (CIA). **A,** Incidence and severity of CIA in 2 experiments. The CIA induction protocol resulted in a high incidence of arthritis, but with variable severity and time to onset (n = 15 mice in each experiment). Values are the percent incidence and the mean arthritis severity score. **B,** Synovial thickness in mice with CIA. Sagittal sections of formalin-fixed hind ankles from 14 animals with CIA and 4 nonarthritic animals were assessed microscopically with a size-calibrated field of view for synovial thickness, and by immunohistochemistry for von Willebrand factor (vWF)–positive vascular density. After development of CIA, the synovium continued to proliferate markedly until frank joint destruction occurred. Synovial neovascularization was extensive in this model. Synovial vWF+ microvessel density peaked 2–3 weeks after symptom onset but declined thereafter, as pannus growth outpaced new vessel formation. For synovial thickness, linear regression analysis yielded a goodness-of-fit (r^2) value of 0.815. The microvascular density curve was generated by third-order polynomial nonlinear regression analysis ($r^2 = 0.746$). Each symbol represents an individual animal. **C–E,** Immunohistochemistry analysis of the synovium of mice with CIA, stained with isotype-matched control antibody (left panels) or target molecule–specific antibody (right panels). Extensive networks of both vWF+ blood vessels (**C**) and LYVE-1+ lymphatic vessels (**D**) are seen, and the inflammatory infiltrate contains large numbers of CD117+ putative endothelial progenitor cells (**E**). **Arrowheads** indicate staining with fast red substrate.

tion markers CD3, CD4, CD8, CD14, and CD19 (results not shown).

Synovial neovascularization in CIA. In the CIA model, arthritis incidence was nearly 100%, with disease severity ~50% of the maximum possible (Figure 1A). Over time, the inflamed synovium thickened (Figure 1B) and became heavily neovascularized (Figure 1C). Included in the synovial inflammatory infiltrate were numerous CD117+ putative EPCs (Figure 1E).

Flow cytometry revealed a mean ± SEM 22 ±

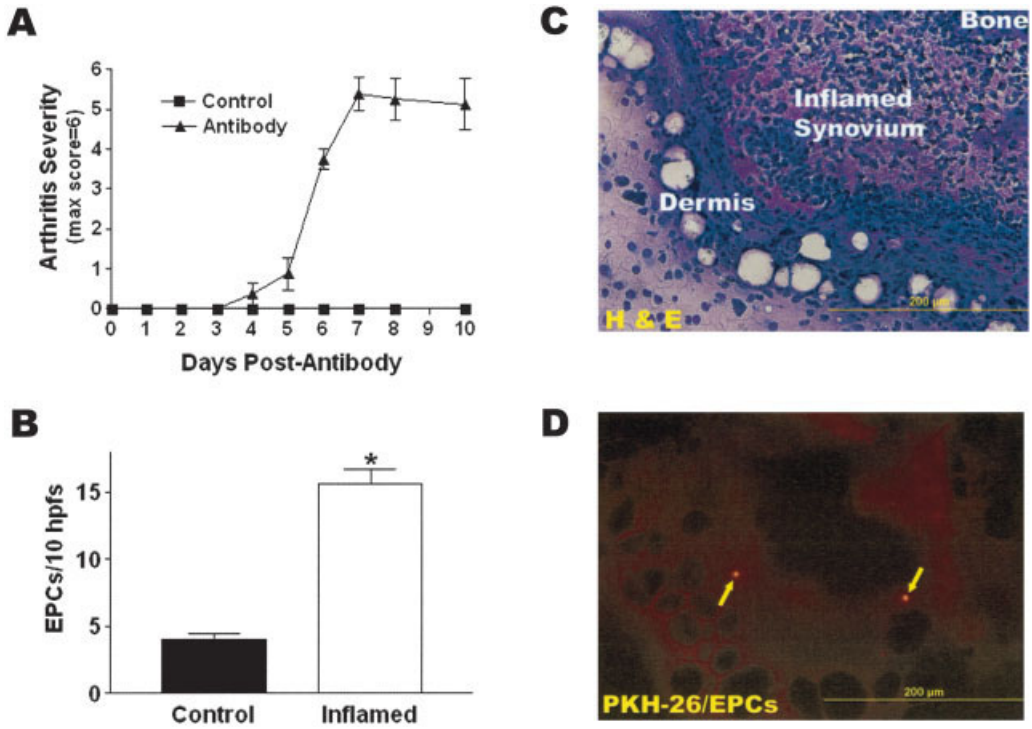

Figure 2. Preferential homing of endothelial progenitor cells (EPCs) to the inflamed synovium in antibody-induced arthritis. Arthritis was elicited in BALB/c mice, using a cocktail of 4 monoclonal antibodies against type II collagen on day 0, followed by intraperitoneal injection of lipopolysaccharide on day 3. EPCs derived from BALB/c mice were injected on day 4 (the day before symptoms generally appear) and were circulated for 5 days. Disease severity in the hind limbs was scored daily. After the mice were killed, the hind limbs were cryosectioned and synovial EPCs were enumerated by fluorescence microscopy. **A,** Mean ± SEM arthritis scores (n = 8 antibody-treated mice [6 of which were used in subsequent EPC homing studies] and 6 controls). **B,** Number of EPCs per high-power field (hpf) in the tibial/tarsal synovial region of arthritic ankles compared with noninflamed control ankles. Values are the mean and SEM (n = 6 mice per group). $* = P < 0.05$ versus controls, by Student's *t*-test. **C** and **D**, Typical hematoxylin and eosin (H&E)–stained (**C**) and fluorescence (**D**) micrographs of serial sections of inflamed ankles. **Arrows** indicate dye-tagged EPCs in the synovial inflammatory infiltrate. Color figure can be viewed in the online issue, which is available at http://www.arthritisrheum.org.

4% increase in Sca-1+ cells in the lymphocytic gate of peripheral blood from animals with arthritis (n = 6) versus control animals (n = 4) ($P < 0.05$). In addition to formation of new vWF+ synovial blood vessels, we observed the establishment of new LYVE-1+ synovial lymphatic vessels (Figure 1D). Synovial thickening progressed such that at 1 month post–symptom onset, the synovium at the tibial/tarsal juxtaposition was nearly 10-fold thicker in arthritic animals than in nonarthritic control animals (from a mean ± SEM of 56 ± 11 μm thick in control animals to 470 ± 24 μm in arthritic animals; $P < 0.05$). Normal synovial vascularization was sparse (35 ± 8 vWF+ vessels/mm^2), but vessel density increased rapidly with disease progression, peaking at ~2–3 weeks post–symptom onset (330 ± 60 vessels/mm^2; $P < 0.05$ versus nonarthritic controls), and then declined as synovial proliferation outpaced neovascularization. Thus, in this arthritis model we found EPC mobilization and accumulation in the arthritic joint lining, which was coincident with enhanced synovial neovascularization.

Homing of EPCs to the inflamed synovium in antibody-induced arthritis. We used the anti–type II collagen antibody–induced arthritis model (10) to investigate homing of exogenously administered EPCs to synovium at arthritis onset. Murine Lin− EPCs were injected on the day before predicted symptom onset and were evaluated in joints 5 days later, when inflammation was maximal. Disease incidence was nearly 100% with this model, with arthritis severity in the hind limbs approaching 90% of maximal (Figure 2A), although disease severity in the front limbs was ~50% of maximal (data not shown). Thus, we analyzed EPC homing to synovium from the hind ankle. In mouse hind ankles, we

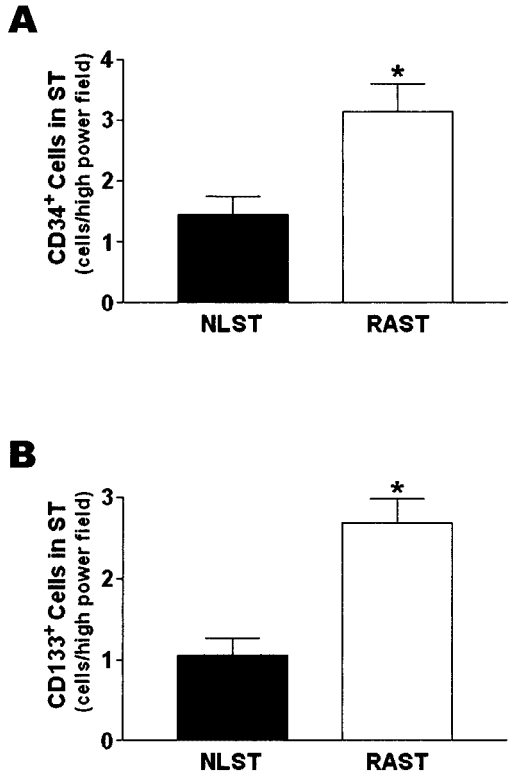

Figure 3. Selective recruitment of endothelial progenitor cells (EPCs) to rheumatoid arthritis (RA) versus normal human synovium in a human/SCID mouse chimera model. RA synovial tissue (RA ST) or normal ST (NLST) was engrafted subcutaneously into SCID mice. Fifteen days after implantation (CD34 experiment) (**A**) or 18 days after implantation (CD133 experiment) (**B**), 1×10^6 fluorescence-labeled human CD34+ hematopoietic progenitor cells or CD133+ EPCs were injected intravenously, and were allowed to circulate for 2 days prior to graft recovery and evaluation. EPCs in cryosections of nonfibrous regions of synovial grafts were enumerated using a fluorescence microscope. Both CD34+ progenitor cells and CD133+ EPCs were selectively localized to RA ST compared with normal ST. Values are the mean and SEM (n = 4–6 mice per group). $*$ = $P < 0.05$ versus normal ST, by Student's *t*-test.

observed a 4-fold increase in the number of synovial EPCs in arthritic animals versus controls (n = 6 animals per group) (mean ± SEM 15.6 ± 1.1 versus 4.0 ± 0.5 EPCs/10hpf; $P < 0.05$) (Figure 2B). Thus, EPCs selectively homed to inflamed synovium. Figures 2C and D show typical hematoxylin and eosin–stained and fluorescence micrographs of serial sections of inflamed ankles.

Selective homing of EPCs to RA ST in the SCID/human ST chimera model. After 2 days of EPC circulation, we evaluated the recruitment of fluorescence-labeled EPCs to RA ST and normal ST that had been engrafted into SCID mice. We observed significantly increased recruitment of human CD34+ cells to RA ST versus normal ST grafts (n = 5 animals per group) (mean ± SEM 3.2 ± 0.4 versus 1.4 ± 0.3 cells/hpf; $P < 0.05$) (Figure 3A). In another experiment using human CD133+ cells, a more specific marker for EPCs than CD34 expression alone (11), we observed a nearly 3-fold increase in EPC recruitment to RA versus normal human ST (n = 5 animals per group) (2.7 ± 0.3 versus 1.1 ± 0.2 EPCs/hpf; $P < 0.05$) (Figure 3B). Thus, in this in vivo model, human EPCs were selectively recruited by inflamed human synovium compared with normal ST.

TNFα-induced up-regulation of VCAM-1 and ICAM-1 expression in RA ST fibroblasts. We observed both time- and concentration-dependent up-regulation of VCAM-1 and ICAM-1 in TNFα-stimulated RA ST fibroblasts (Figure 4). Activation for 24 hours with 20 ng/ml TNFα resulted in a mean ± SEM 4.8 ± 1.4–fold increase in ICAM-1, and a 10.4 ± 1.8–fold increase in VCAM-1 surface expression on RA ST fibroblasts, evaluated by enzyme-linked immunocellular assay (n = 3 experiments). The mean 50% maximum response concentration was ~300 pg/ml TNFα for ICAM-1 induction and ~3 ng/ml TNFα for VCAM-1 induction. Both CAMs showed significant induction with TNFα starting at a concentration of 200 pg/ml. Western blotting of RA ST fibroblast lysates from cells treated with 20 ng/ml TNFα revealed significant induction beginning at 4 hours with both CAMs. ICAM-1 up-regulation was maximal at 6 hours and began declining by 24 hours (Figure 4C). VCAM-1 up-regulation was maximal at 4 hours and was maintained at this level through ≥24 hours (Figure 4D).

Mediation of EPC adhesion to cultured RA ST fibroblasts by VCAM-1/α4 integrin, but not by ICAM-1 or ICAM-2. CD133+ EPCs adhered to TNFα-activated RA ST fibroblasts in both a cytokine concentration–dependent and a time-dependent manner (Figures 5A and B). Increased adhesion was apparent with ~20 pg/ml of TNFα, after 18 hours of stimulation. Higher concentrations of TNFα (i.e., 20 ng/ml) resulted in significantly increased EPC adhesion after 2.5 hours, which continued to increase through ≥20 hours. Anti–VCAM-1 neutralizing antibody completely inhibited TNFα-induced adhesion of EPCs to RA ST fibroblasts, to levels seen with unstimulated RA ST fibroblasts (Figure 5C). Although anti–ICAM-1 or anti–ICAM-2 alone did not inhibit EPC adhesion to activated RA ST fibroblasts, all 3 CAM antibodies combined caused a modest additional inhibitory effect on adhesion compared with anti–VCAM-1 alone. Similarly, blocking antibodies against α4 integrin completely abrogated EPC binding to activated

RA ST fibroblasts, while anti–β2 integrin- and anti–αL integrin alone had no significant effect (Figure 5D). Combined treatment with all 3 integrin antibodies resulted in a modest additional inhibition of EPC adhesion, compared with that seen with anti–α4 integrin alone. These data demonstrate that the VCAM-1/very late activation antigen 4 (VLA-4) ligand/receptor pair critically mediates EPC adhesion interactions with RA ST fibroblasts.

Mediation of EPC adhesion to human RA ST cryosections by VCAM-1/α4 integrin. EPC binding to cultured RA ST fibroblasts is primarily dependent on VCAM-1 and the VLA-4 integrin subunit α4. We sought to elucidate the contributions of these molecules to EPC adhesion to a more heterogeneous substratum, i.e., inflamed human RA ST (Figure 6). Anti–VCAM-1 and anti–α4 integrin antibodies caused significant inhibition of EPC adhesion to RA ST (mean ± SEM 43 ± 3% and 53 ± 13%, respectively, of the level of EPC binding to control antibody–treated RA ST). This suggests that VCAM-1 and VLA-4 have a major role in mediating EPC recruitment to inflamed synovium.

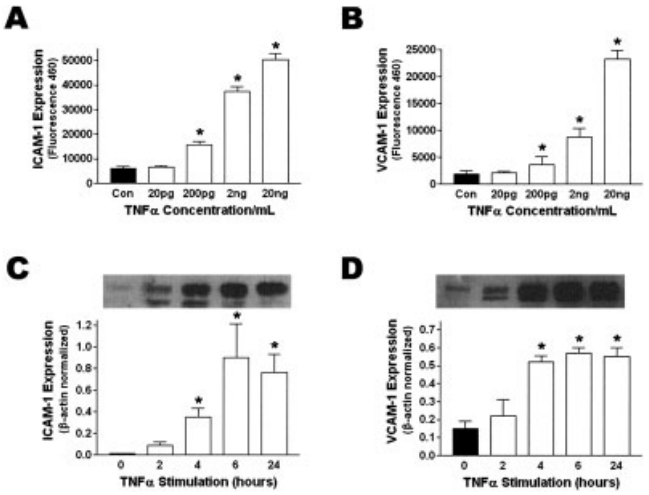

Figure 4. Intercellular adhesion molecule 1 (ICAM-1) and vascular cell adhesion molecule 1 (VCAM-1) functional and protein expression in cytokine-activated rheumatoid arthritis synovial tissue (RA ST) fibroblasts. RA ST fibroblasts were stimulated with tumor necrosis factor α (TNFα) for up to 24 hours and were then evaluated by enzyme-linked immunocellular assay (**A** and **B**) or Western blotting (**C** and **D**). Both ICAM-1 and VCAM-1 were strongly up-regulated by TNFα, in both a concentration-dependent manner (24-hour stimulation) (**A** and **B**) and a time-dependent manner (20 ng/ml TNFα) (**C** and **D**). Data shown are from 1 representative experiment of 3 independent experiments conducted with RA ST fibroblasts from different donors (4–6 replicates per group in enzyme-linked immunocellular assays, and duplicate lanes in Western blots). Values are the mean and SEM (bar graphs in **C** and **D** represent quantitation of the Western blot results). $* = P < 0.05$ versus unstimulated controls (Con), by Student's *t*-test.

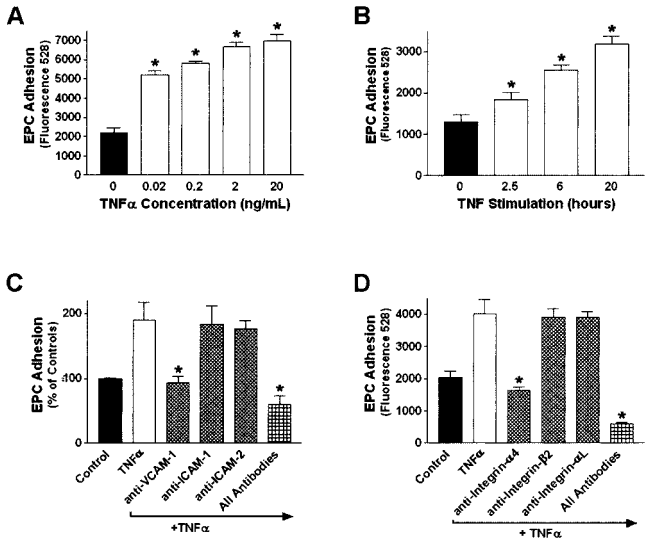

Figure 5. Mediation of endothelial progenitor cell (EPC) adhesion to activated RA ST fibroblasts by VCAM-1/α4 integrin interactions, but not ICAM-1 or -2. TNFα induced RA ST fibroblasts to bind EPCs, in both a concentration-dependent manner (18-hour stimulation) (**A**) and a time-dependent manner (20 ng/ml TNFα) (**B**). Inclusion of neutralizing antibodies against VCAM-1 completely abrogated TNFα-induced (20 ng/ml, 18 hours) adhesion of EPCs to RA ST fibroblasts, while inhibition of ICAM-1 or ICAM-2 activity alone had no significant effect on EPC binding (**C**). Anti–α4 integrin also completely negated TNFα-induced (20 ng/ml, 18 hours) adhesion of EPCs to RA ST fibroblasts, while inhibition of β2 integrin or αL integrin activity individually had no significant effect on EPC adhesion (**D**). Neutralizing antibodies were used at 10 μg/ml and remained in the assay media throughout the attachment period. Data shown are from 1 representative experiment of 3 independent experiments conducted with RA ST fibroblasts from different donors (4–6 replicates per group). Values are the mean and SEM. $* = P < 0.05$ versus no stimulation (**A** and **B**) or versus TNFα treatment alone (**C** and **D**), by Student's *t*-test. See Figure 4 for other definitions.

DISCUSSION

EPCs were first identified in the adult circulation in 1999 (12). Since then, bone marrow–derived EPCs have been shown to play a role in the neovascularization that occurs in diverse damaged and diseased tissues (13–16). EPCs comprise a subset of the CD34+ hematopoietic stem cell bone marrow fraction (17). In humans, the best EPC marker is the orphan tetraspan protein CD133 (11). In mice, the best marker profile for EPCs identified so far is CD117+,Sca-1+ double-positive, with no detectable expression of leukocyte maturation markers (Lin−) (18,19). Given the extensive

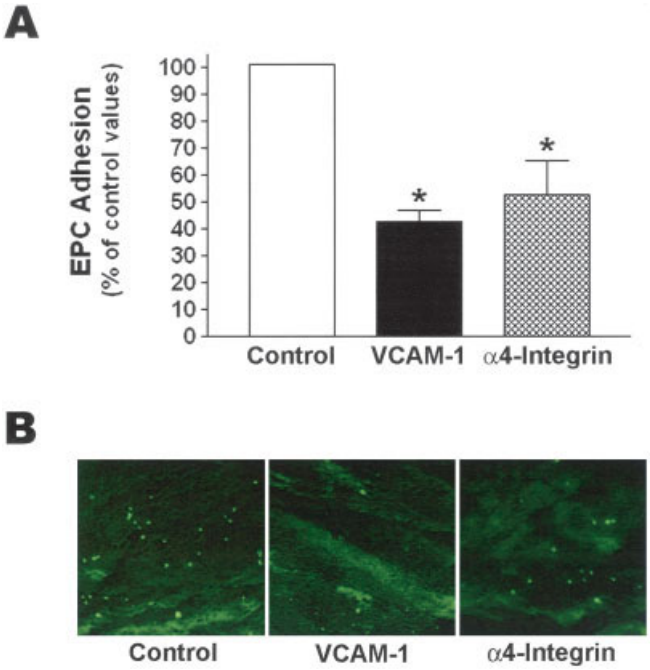

Figure 6. Mediation of EPC adhesion to RA ST by vascular cell adhesion molecule 1 (VCAM-1)/α4 integrin interactions. Fluorescence-labeled human EPCs were incubated on rehydrated RA ST cryosections. After 20 minutes, nonattached EPCs were washed off and adherent cells were enumerated. **A,** EPC binding after inclusion of neutralizing antibodies against either VCAM-1 or α4 integrin in the adhesion media. All antibodies were used at 10 μg/ml and remained in the adhesion media throughout the attachment period. Addition of VCAM-1 or α4 integrin neutralizing antibodies resulted in similar ~50% inhibition of EPC binding compared with sections that were incubated with isotype-matched control antibody. RA ST was from 6 different donors in the VCAM-1 studies and from 8 different donors in the α4 integrin studies. Values are the mean and SEM. $* = P < 0.05$ versus control, by Student's *t*-test. **B,** Fluorescence microscopy, showing typical patterns of EPC adhesion to RA ST cryosections treated with neutralizing antibodies against VCAM-1 or α4 integrin, or isotype-matched control antibody (original magnification $\times$ 200). See Figure 3 for other definitions. Color figure can be viewed in the online issue, which is available at http://www.arthritisrheum.org.

neovascularization that occurs in RA, we hypothesized that EPCs are recruited to the arthritic synovium, where they might contribute to expansion of the synovial microcirculation.

One primary finding in our study was that, in 3 diverse animal models used to investigate cell homing in arthritis, EPCs preferentially localized to inflamed synovium compared with normal synovium. The murine CIA model is characterized by marked synovial neovascularization (including lymphatic vessels) that is measurable within days of symptom onset. Microvascular density is maximal ~2–3 weeks after arthritis onset, after which it declines as synovial pannus growth outpaces new vessel formation. In CIA, this hyperproliferative synovium invades the joint cartilage and underlying bone, ultimately causing frank joint destruction, typically $\geq$3 weeks after onset of clinical symptoms. We speculate that neovascularization slows even while the pannus continues to enlarge, because the invasive synovium begins acquiring necessary additional nutrients and oxygen from the marrow cavities of the newly eroded bone.

In the CIA model, we observed CD117+ cells in the inflammatory infiltrate of arthritic joints, whereas we did not detect cells bearing this EPC marker in the joint lining of control animals. This correlates well with earlier observations that the number of EPCs per mm^2 identified immunohistologically in postsurgical human RA ST samples was elevated ~25-fold over the number of EPCs localized in normal ST (6).

We also observed increased numbers of Sca-1+ cells in the lymphocytic fraction of the peripheral blood mononuclear cells of mice with established CIA. In an earlier study that used a similar CIA model, EPCs were also elevated in the peripheral blood of mice at the time of disease onset (20). However, in that study, EPCs were not elevated prior to the onset of clinically identifiable symptoms or 1 week after arthritis was established, when disease severity scores were maximal. In contrast, we found that EPCs were significantly elevated 2–21 days post–inflammation onset in animals with arthritis. This difference could be due to the use of slightly different CIA induction protocols, or could reflect the fact that CD117 was used as the EPC-defining marker in the earlier study (20), whereas we used Sca-1 for EPC identification in peripheral blood. Nonetheless, taken together these data suggest that EPCs are mobilized into the circulation during arthritis pathogenesis, are recruited to the inflamed synovium, and may contribute to disease progression.

In contrast to the above-mentioned observations of elevated circulating EPC levels in mouse arthritis models, studies in humans have shown that EPCs are decreased in the peripheral blood of patients with active RA compared with healthy individuals (21,22). Depletion of EPCs from the circulation in RA patients with established disease reflects their enhanced extravasation out of the bloodstream and into the inflamed joint.

We used 2 other in vivo models to track exogenously administered EPCs to inflamed synovial tissue in mice. In an anticollagen antibody–induced arthritis model, murine EPCs accumulated preferentially in inflamed joint lining, and were only rarely observed in the vicinity of unaffected joints. In a human ST/SCID mouse

chimera, exogenous human EPCs that were injected into ST-engrafted mice selectively accumulated in RA ST compared with normal human synovial grafts. Although these models do not entirely replicate the mechanistic complexities of human RA, they certainly demonstrate that EPCs are recruited to inflamed joint tissue.

We sought to elucidate the mechanisms of the egress of EPCs into inflamed synovium. The inflammatory cytokine TNFα is highly expressed in RA joints (23), and clinical strategies to target TNFα have demonstrated its importance in RA (24). TNFα induces many cell types, including RA ST fibroblasts, to express adhesion molecules and chemokines that recruit leukocytes (25). We used an in vitro adhesion assay to assess the contribution of specific adhesion molecules to CD133+ EPC adhesion to TNFα-activated RA ST fibroblasts and to RA ST cryosections. Treatment of RA ST fibroblasts with TNFα confirmed the previously described concentration- and time-dependent induction of ICAM-1 and VCAM-1 expression on RA ST fibroblasts (26), as well as the concomitant increase in adhesiveness of RA ST fibroblasts for EPCs. Studies with neutralizing antibodies demonstrated the primary importance of RA ST fibroblast–expressed VCAM-1, but not ICAM-1 or -2, in mediating EPC–RA ST fibroblast binding.

Given that the vast majority of EPCs express the VCAM-1 counterreceptor (VLA-4) subunit, α4 integrin, we tested whether antibodies against α4 integrin, or other integrins, would inhibit EPC adhesion to TNFα-activated RA ST fibroblasts. We observed total abrogation of EPC–RA ST fibroblast binding, to levels observed in control experiments using unstimulated RA ST fibroblasts, when anti–α4 integrin antibody was included in the adhesion assay. Inhibition of αL integrin (a subunit of the ICAM-1/2 receptor lymphocyte function–associated antigen 1 [LFA-1]) or of β2 integrin (a common subunit of LFA-1 and also of the ICAM-1/2 receptor Mac-1), present on certain leukocytes (27), had no effect on EPC–RA ST fibroblast adhesion. In experiments in which EPC adhesion to cryosections of RA ST was evaluated, we found a >50% decrease in EPC adhesion to RA ST sections when either anti–VCAM-1 or anti–α4 integrin antibodies were included in the assay. Together, these results provide evidence of a major role of the VCAM-1/VLA-4 adhesion system, but not the ICAM/LFA-1 system, in mediating EPC accumulation in inflamed joint tissue.

There are multiple similarities among the physical environments in arthritic joints, ischemia-damaged muscle, and solid tumors (e.g., hypoxia, acidification, and expression of inflammatory and angiogenic mediators) (28). VCAM-1 expression is up-regulated in all of these conditions (29–31), and all of these tissues recruit EPCs (15,32–35). The mechanisms by which EPCs home to these tissues, however, remain poorly elucidated. In RA models, VCAM-1 regulates B lymphocyte influx into (36), and survival within (37), the joint. Recently it was demonstrated that recruitment of CD34+ hematopoietic stem cells, the parent population of CD133+ EPCs, into the neovasculature of tumors utilizes the VCAM-1/VLA-4 adhesive system (38). EPCs are recruited to ischemia-damaged muscle to reconstitute a functional microcirculation (32), and ICAM-1 plays a primary role in EPC recruitment to muscle (39). Ours is the first study to define the specific participation of the VCAM-1/VLA-4 system, but not the ICAM/β2 integrin subunit pair, in mediating EPC interactions with synovial cells. This suggests that the selective use of distinct adhesion molecules plays a role in recruitment of EPCs to the synovium during human RA pathogenesis, and highlights the mechanistic differences in EPC recruitment in diverse disease states.

By understanding the mechanisms of EPC recruitment, we can regulate EPC function in humans. In conditions such as myocardial damage, the goal is to enhance EPC contributions to neovascularization, with the desired result of revitalizing the blood supply to the compromised heart. In the cases of tumorigenesis and RA, the opposite effect, inhibition of neovascularization in order to starve and thus inhibit the expansion of invasive tissue, is the desired effect. A clearer understanding of the biologic processes that guide EPCs to the microcirculatory beds of inflamed and angiogenic tissue could lead to the development of new tools with which to modulate these activities.

ACKNOWLEDGMENTS

We thank Patricia Chang, J. J. Ren, and Naveena Reddy for their technical input.

AUTHOR CONTRIBUTIONS

Dr. Silverman had full access to all of the data in the study and takes responsibility for the integrity of the data and the accuracy of the data analysis.

Study design. Silverman, Haas, Arbab, Koch.

Acquisition of data. Silverman, Haas.

Analysis and interpretation of data. Silverman, Haas, Rad, Arbab, Koch.

Manuscript preparation. Silverman, Koch.

Statistical analysis. Silverman, Haas.

Isolation/characterization of endothelial progenitor cells. Silverman, Rad, Arbab.

REFERENCES

1. Koch AE. Angiogenesis as a target in rheumatoid arthritis. Ann Rheum Dis 2003;62 Suppl 2:ii60–7.
2. Folkman J, Haudenschild C. Angiogenesis in vitro. Nature 1980; 288:551–6.
3. Patan S. Vasculogenesis and angiogenesis. Cancer Treat Res 2004;117:3–32.
4. Masuda H Asahara T. Post-natal endothelial progenitor cells for neovascularization in tissue regeneration. Cardiovasc Res 2003;58: 390–8.
5. Paleolog EM. Angiogenesis in rheumatoid arthritis. Arthritis Res 2002;4 Suppl 3:S81–90.
6. Ruger B, Giurea A, Wanivenhaus AH, Zehetgruber H, Hollemann D, Yanagida G, et al. Endothelial precursor cells in the synovial tissue of patients with rheumatoid arthritis and osteoarthritis. Arthritis Rheum 2004;50:2157–66.
7. Myers LK, Rosloniec EF, Cremer MA, Kang AH. Collagen-induced arthritis, an animal model of autoimmunity. Life Sci 1997;61:1861–78.
8. Kanda K, Hayman GT, Silverman MD, Lelkes PI. Comparison of ICAM-1 and VCAM-1 expression in various human endothelial cell types and smooth muscle cells. Endothelium 1998;6:33–44.
9. Stamper HB Jr, Woodruff JJ. An in vitro model of lymphocyte homing. I. Characterization of the interaction between thoracic duct lymphocytes and specialized high-endothelial venules of lymph nodes. J Immunol 1977;119:772–80.
10. Terato K, Hasty KA, Reife RA, Cremer MA, Kang AH, Stuart JM. Induction of arthritis with monoclonal antibodies to collagen. J Immunol 1992;148:2103–8.
11. Yin AH, Miraglia S, Zanjani ED, Almeida-Porada G, Ogawa M, Leary AG, et al. AC133, a novel marker for human hematopoietic stem and progenitor cells. Blood 1997;90:5002–12.
12. Asahara T, Masuda H, Takahashi T, Kalka C, Pastore C, Silver M, et al. Bone marrow origin of endothelial progenitor cells responsible for postnatal vasculogenesis in physiological and pathological neovascularization. Circ Res 1999;85:221–8.
13. Shi Q, Rafii S, Wu MH, Wijelath ES, Yu C, Ishida A, et al. Evidence for circulating bone marrow-derived endothelial cells. Blood 1998;92:362–7.
14. Kalka C, Masuda H, Takahashi T, Kalka-Moll WM, Silver M, Kearney M, et al. Transplantation of ex vivo expanded endothelial progenitor cells for therapeutic neovascularization. Proc Natl Acad Sci U S A 2000;97:3422–7.
15. Lyden D, Hattori K, Dias S, Costa C, Blaikie P, Butros L, et al. Impaired recruitment of bone-marrow-derived endothelial and hematopoietic precursor cells blocks tumor angiogenesis and growth. Nat Med 2001;7:1194–201.
16. Lee IG, Chae SL, Kim JC. Involvement of circulating endothelial progenitor cells and vasculogenic factors in the pathogenesis of diabetic retinopathy. Eye 2006;20:546–52.
17. D'Arena G, Savino L, Nunziata G, Cascavilla N, Matera R, Pistolese G, et al. Immunophenotypic profile of AC133-positive cells in bone marrow, mobilized peripheral blood and umbilical cord blood. Leuk Lymphoma 2002;43:869–73.
18. Okada S, Nakauchi H, Nagayoshi K, Nishikawa S, Miura Y, Suda T. In vivo and in vitro stem cell function of c-kit- and Sca-1-positive murine hematopoietic cells. Blood 1992;80:3044–50.
19. Li TS, Hamano K, Nishida M, Hayashi M, Ito H, Mikamo A, et al. CD117+ stem cells play a key role in therapeutic angiogenesis induced by bone marrow cell implantation. Am J Physiol Heart Circ Physiol 2003;285:H931–7.
20. Kurosaka D, Yasuda J, Yoshida K, Yasuda C, Toyokawa Y, Yokoyama T, et al. Kinetics of circulating endothelial progenitor cells in mice with type II collagen arthritis. Blood Cells Mol Dis 2005;35:236–40.
21. Grisar J, Aletaha D, Steiner CW, Kapral T, Steiner S, Seidinger D, et al. Depletion of endothelial progenitor cells in the peripheral blood of patients with rheumatoid arthritis. Circulation 2005;111: 204–11.
22. Herbrig K, Haensel S, Oelschlaegel U, Pistrosch F, Foerster S, Passauer J. Endothelial dysfunction in patients with rheumatoid arthritis is associated with a reduced number and impaired function of endothelial progenitor cells. Ann Rheum Dis 2006;65:157–63.
23. Feldmann M, Brennan FM, Maini RN. Role of cytokines in rheumatoid arthritis. Annu Rev Immunol 1996;14:397–440.
24. Puppo F, Murdaca G, Ghio M, Indiveri F. Emerging biologic drugs for the treatment of rheumatoid arthritis. Autoimmun Rev 2005;4:537–41.
25. McMurray RW. Adhesion molecules in autoimmune disease. Semin Arthritis Rheum 1996;25:215–33.
26. Marlor CW, Webb DL, Bombara MP, Greve JM, Blue ML. Expression of vascular cell adhesion molecule-1 in fibroblastlike synoviocytes after stimulation with tumor necrosis factor. Am J Pathol 1992;140:1055–60.
27. Fabbri M, Bianchi E, Fumagalli L, Pardi R. Regulation of lymphocyte traffic by adhesion molecules. Inflamm Res 1999;48: 239–46.
28. Polverini PJ. Angiogenesis in health and disease: insights into basic mechanisms and therapeutic opportunities. J Dent Educ 2002;66:962–75.
29. Matsuyama T, Kitani A. The role of VCAM-1 molecule in the pathogenesis of rheumatoid synovitis. Hum Cell 1996;9:187–92.
30. Tousoulis D, Homaei H, Ahmed N, Asimakopoulos G, Zouridakis E, Toutouzas P, et al. Increased plasma adhesion molecule levels in patients with heart failure who have ischemic heart disease and dilated cardiomyopathy. Am Heart J 2001;141:277–80.
31. Johnson JP. Cell adhesion molecules in the development and progression of malignant melanoma. Cancer Metastasis Rev 1999; 18:345–57.
32. Ott I, Keller U, Knoedler M, Gotze KS, Doss K, Fischer P, et al. Endothelial-like cells expanded from CD34+ blood cells improve left ventricular function after experimental myocardial infarction. FASEB J 2005;19:992–4.
33. Otsuki M, Hashimoto K, Morimoto Y, Kishimoto T, Kasayama S. Circulating vascular cell adhesion molecule-1 (VCAM-1) in atherosclerotic NIDDM patients. Diabetes 1997;46:2096–101.
34. Otani A, Kinder K, Ewalt K, Otero FJ, Schimmel P, Friedlander M. Bone marrow-derived stem cells target retinal astrocytes and can promote or inhibit retinal angiogenesis. Nat Med 2002;8: 1004–10.
35. Kawamoto A, Tkebuchava T, Yamaguchi J, Nishimura H, Yoon YS, Milliken C, et al. Intramyocardial transplantation of autologous endothelial progenitor cells for therapeutic neovascularization of myocardial ischemia. Circulation 2003;107:461–8.
36. Burger JA, Zvaifler NJ, Tsukada N, Firestein GS, Kipps TJ. Fibroblast-like synoviocytes support B-cell pseudoemperipolesis via a stromal cell-derived factor-1- and CD106 (VCAM-1)-dependent mechanism. J Clin Invest 2001;107:305–15.
37. Shimaoka Y, Attrep JF, Hirano T, Ishihara K, Suzuki R, Toyosaki T, et al. Nurse-like cells from bone marrow and synovium of patients with rheumatoid arthritis promote survival and enhance function of human B cells. J Clin Invest 1998;102:606–18.
38. Jin H, Aiyer A, Su J, Borgstrom P, Stupack D, Friedlander M, et al. A homing mechanism for bone marrow-derived progenitor cell recruitment to the neovasculature. J Clin Invest 2006;116: 652–62.
39. Yoon CH, Hur J, Oh IY, Park KW, Kim TY, Shin JH, et al. Intercellular adhesion molecule-1 is upregulated in ischemic muscle, which mediates trafficking of endothelial progenitor cells. Arterioscler Thromb Vasc Biol 2006;26:1066–72.